Citation
Datta, A. and Ghosh, A. and Rajakaruna, S. 2017. Power sharing in a hybrid microgrid with bidirectional switch, 2017 IEEE Power & Energy Society General Meeting, Chicago, IL, USA, pp. 1-5. http://doi.org/10.1109/PESGM.2017.8274281

Power Sharing in a Hybrid Microgrid with Bidirectional Switch

Amit Jyoti Datta, *Student Member IEEE*; Arindam Ghosh, *Fellow, IEEE*; Sumedha Rajakaruna, *Senior Member, IEEE* Dept. of Electrical and Computer Engineering
Curtin University, Bentley, WA, Australia

***Abstract*— The main aim of this study is to facilitate controlled power flow in a hybrid microgrid (MG) containing an AC and a DC side. These two sides are connected through an interlinking converter (IC). It has been assumed that distributed generators (DGs) in the AC side and the DC side supply their local loads through AC and DC droops respectively. During a power shortfall in one of the two sides, the required amount of is drawn from the other side through the interlinking converter. A new approach is proposed in this paper in which power shortfall is detected in the ac side though frequency and by voltage in the dc side. The IC is then controlled such that bi-directional power flow can be achieved. Simulation studies are conducted on PSCAD/EMTDC to validate the proposal.**

***Index Terms*— Hybrid microgrid, droop coefficient, interlinking converter.**

I. INTRODUCTION

Fossil energy sources have been the major source for electric power generation for a long time. However to reduce the carbon emission from these fossil fuel based power generators and at the same time to ensure a reliable and flexible energy source, renewable energy based power generation are currently gaining much attention. In this regard, distributed generation (DG) based on renewable sources, which are located near the distribution network or connected directly to the customer site of the meter [1, 2], are getting connected to power distribution networks. Also microgrids containing several DGs can provide a better control flexibility to maintain a stable operation for a cluster of loads and paralleled DG systems [3-6].

A hybrid microgrid (MG) contains an AC side and a DC side, each of which operate independent of the other through their own droop for real power sharing. These two sides are linked together through an interlinking AC/DC converter, which can facilitate a bi-directional power flow. A large majority of electrical loads, such as LED-lighting, adjustable speed motors, electric vehicles, computing and communication equipment need dc supply. At the same time, many DERs like PV, batteries, fuel cell produce power at dc voltage level, which is then converted in ac for grid connection. In order to avoid the conversion losses, DC microgrids are gaining increased attention these days. Voltage transformation in a DC grid is achieved through DC-DC converters, which have 95% efficiency. However, when AC loads coexist with DC loads, hybrid microgrids can be considered [7-10].

Usually, the DGs in a MG are scattered in a region which makes it inconvenient to establish a power sharing via a communication link with wires. Subsequently, the droop control method has been adapted by many researchers to determine the electric power contribution of each DGs for load demand sharing [7-10]. This power sharing is achieved in the proportion to the power ratings of the DGs [8]. Power sharing in the AC side of the hybrid microgrid could be controlled by regulating the frequency to a desired range, where the DC side power distribution is voltage dependent. Subsequently, during coupling of the AC microgrid and the DC microgrid, the major challenge for controlling the power sharing is the mismatch of the droop coefficients of the interlinking converter [10]. Normalization of the droop equations [10] and a technique considering AC side frequency and DC side voltage as a common signal to generate droop coefficients for the interlinking converter has been adopted in the existing research [11].

In this article, a power flow control switch has been introduced in the DC side of the IC to control the power flow between the AC and the DC MGs. This bidirectional switch controls the power flow in a hybrid microgrid based only on the local measurement. In this, the desired amount of power required to flow is computed from the frequency in the AC side and the voltage in the DC side. It will be shown how these signals can be used for overload prevention of the either side.

II. SYSTEM STRUCTURE AND DROOP CONTROL

The simple hybrid microgrid structure considered in this study is shown in Fig. 1. In this, both the AC and DC sides form two separate microgrids that operate independent of each other. They however transfer power through the interlinking converter only when one of the microgrids has a power shortfall. The IC regulates the voltage across the DC capacitor C_{dc} according to the power flow requirement. The switch pairs S_1 and S_2 are normally open. One of them closes to facilitate power transfer in the required direction only when a command is issued. For example, when the AC-MG needs to supply power to the DC-MG, S_1 closes. Alternatively S_2 closes when the DC-MG supplies power to the AC-MG. The switching strategy is discussed in the next section.

A. AC-MG Droop Control

The DGs in the AC-MG is controlled in a decentralized manner through P-f and Q-V droop, given by

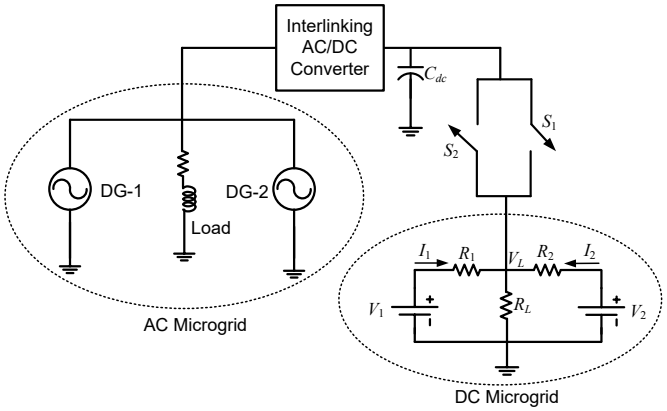

Fig. 1. A compact representation of the proposed hybrid grid.

$$f = f_r + m \times \left(0.5P^* - P\right) \tag{1}$$

$$V = V_r + n \times (Q^* - Q) \tag{2}$$

where f_r and f are the rated and instantaneous frequency of the system respectively. The rated and actual real power are denoted by P^* and P respectively; Q^* and Q are the rated and actual reactive power respectively. m, n are the droop coefficients of the frequency and voltage droop lines.

The droop gain is such chosen that the frequency deviation is restricted to $\pm\Delta f$ from the reference frequency f_r, which is taken as 50 Hz. The droop gain then can be determined from [12]

$$m = \frac{\Delta f}{0.5P^*} \tag{3}$$

When all the DGs in the MG follow (3) to compute their droop gains according to their power ratings, we get

$$m_1 \times P_1^* = m_2 \times P_2^* = \cdots = m_N \times P_N^* \tag{4}$$

where N is the total number of DGs in the AC-MG.

B. DC-MG Droop Control

Consider the DC-MG of Fig. 1, which contains only two DGs. In this, the dc sources have voltages of V_1 and V_2, the feeder resistances are denoted by R_1 and R_2. These sources supply a resistive load R_L. The droop equations for a dc microgrid are given by

$$V_1 = V_{ref} - d_1 I_1, \quad V_2 = V_{ref} - d_2 I_2 \tag{5}$$

where d_1 and d_2 are the droop gains. Then under the assumption $d_1 >> R_1$ and $d_2 >> R_2$, the power sharing between the two DGs is given by the equation

$$\frac{P_1}{P_2} \approx \frac{d_2}{d_1} \tag{6}$$

where $P_1 = V_1 \times I_1$ and $P_2 = V_2 \times I_2$ are respectively the power supplied by DG-1 and DG-2 in the DC-MG.

It is stipulated that the voltage drop in the DC-MG is restricted to $V_{\min} = V_{ref} - \Delta V$. Therefore from (5), we get

$$\Delta V = V_{ref} - V_{\min} = dI = d\frac{P_{\max}}{V_{\min}} \tag{7}$$

where P_{max} is the maximum power supplied by a DG. Therefore the droop gain is chosen as

$$d = \Delta V \frac{V_{\min}}{P_{\max}} \tag{8}$$

Now if the droop gains of all the DGs in the DC-MG is chosen as per (8), the voltage of all the DGs in the DC-MG will drop to $V_{ref} - \Delta V$ when they are supplying their maximum rated power.

III. Operating Modes

The hybrid microgrid operates in three different modes. These are discussed in this section.

A. Mode-1: Isolated Mode of Operation

In this mode, it has been assumed that the DGS in both the AC and DC MG has sufficient power to supply their respective local loads. In this case, they then supply the loads through the respective droop equations of (1-2) and (5). The interlinking converter hold the DC voltage across C_{dc} to a prespecified value and the switches S_1 and S_2 remain open. The hybrid microgrid remains in this mode when the following two conditions are satisfied.

$$\text{AC-MG}: \sum_{k=1}^{N_{AC}} P_k^* \geq \sum_{k=1}^{M_{AC}} P_{Lk} + P_{Loss}^{AC} \tag{9}$$

$$\text{DC-MG}: \sum_{k=1}^{N_{DC}} P_k^* \geq \sum_{k=1}^{M_{DC}} P_{Lk} + P_{Loss}^{DC} \tag{10}$$

where N is the total number of DGs in an MG and M is total number loads and P_{Loss} is the line loss.

B. Mode-2: Power Shortfall in AC-MG

In this mode, it has been assumed that condition (9) has been violated, while condition (10) still remains satisfied. It is stipulated that the AC-MG should draw the exact amount power that is required to cancel its power shortfall. It is obvious from the droop equation (1) that when all the DGs in the AC-MG are supplying their rated power, the frequency of the microgrid will become $f_r - \Delta f$ Hz. Therefore through a simple frequency measurement at any point of the MG, the overloading can be detected.

The basic aim is to hold the frequency to $f_r - \Delta f$ Hz by drawing power from the other microgrid through the interlinking converter. Based on this argument, a proportional plus integral (PI) controller is designed that set the reference P_{dca}^* for the amount of power to be drawn from the DC-PEH as

$$\begin{aligned} e_f &= f_r - \Delta f - \hat{f} \\ P_{dca}^* &= K_{Pf}\, e_f + K_{If} \int e_f \, dt \end{aligned} \tag{11}$$

where $\hat{f}$ is the microgrid frequency measured or estimated. The block diagram of the overload prevention scheme is shown in Fig. 2. The estimated frequency $\hat{f}$ is compared with a fixed number of $f_r - \Delta f$. If this is greater than 0, then a trigger signal (T_{rga}) is activated. Otherwise the trigger signal remains zero. If $T_{rga} = 1$, the input to the PI controller is e_f as in (11). When the T_{rga} changes from 1 to 0, a one shot Schmitt trigger is used to generate a pulse that will reset the integrator. The

input to the PI controller is then changed to 0 such that P_{dca}^* is zero as no power is required from the DC-MG. Furthermore, when $T_{rga} = 1$, the switch S_2 is closed.

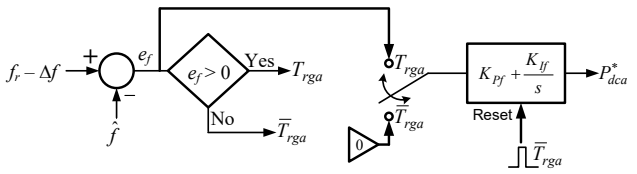

Fig. 2. Schematic diagram of overload prevention in AC-MG.

C. Mode-3: Power Shortfall in DC-MG

In this mode, it has been assumed that condition (10) has been violated, while condition (9) still remains satisfied such that the DC-MG should draw the exact amount power that is required to cancel its power shortfall. As has been discussed in Section II.B, the maximum possible voltage drop in a DG in the DC microgrid is ΔV. Therefore this quantity will be used for overload detection in the DG-MG.

Unlike the AC-MG where the frequency drop can be measured at any point of the network, the voltage drop in the DC-MG has to be measured at one particular DG in the network. Once the voltage drops below the minimum level, a trigger signal (T_{rgb}) is generated, which is then used to close the switch S_1. Thereafter another PI controller is used that holds the voltage at the minimum level and draws the exact amount of power (P_{dcb}^*) from the AC-MG to prevent a collapse in the MG. The PI controller is given by

$$\begin{aligned} e_v &= V_{ref} - \Delta V - V \\ P_{dcb}^* &= K_{Pv}\, e_f + K_{Iv} \int e_v\, dt \end{aligned} \tag{12}$$

The control structure is shown in Fig. 3. This is similar to Fig. 2, where the reset signal is used when the power shortfall is removed.

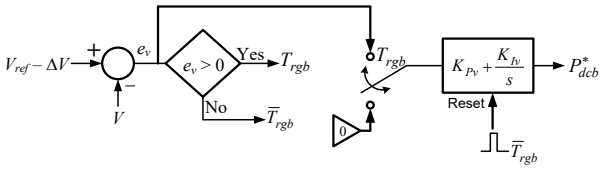

Fig. 3. Schematic diagram of overload prevention in DC-MG.

D. DC Capacitor Votage Reference for IC

Once the reference power P_{dca}^* is computed from (11) or P_{dcb}^* is computed from (12), the voltage across the capacitor C_{dc} has to be changed to facilitate this amount of power flow between the two MGs. The schematic diagram for the capacitor voltage reference generation scheme is shown in Fig. 4. In this the direction of power flowing from the AC-MG to the DC-MG is taken as positive and this power is denoted by P_{dc}. A 4-by-1 multiplexer is used for selecting the correct power reference, as shown in Fig. 4. For example, when s1s0 = 01 (i.e., only T_{rga} is 1), P_{dca}^* is selected as the reference power. On the other hand, when s1s0 = 10 (i.e., only T_{rgb} is 1), $-P_{dcb}^*$ is selected as the reference power (note that this is selected negative due to the chosen direction of power flow). The reference is selected as 0 for s1s0 = 00 or 11. The reference is then compared with the power flowing out of the DC capacitor and is passed through a third PI controller to generate the capacitor voltage reference V_{Lref}. This PI controller is given by

$$\begin{aligned} e_P &= P_{dc}^* - P_{dc} \\ V_{Lref} &= V_{ref} - K_{PP}\, e_P - K_{IP} \int e_P\, dt \end{aligned} \tag{13}$$

The PI controller is reset when either T_{rga} or T_{rgb} becomes zero.

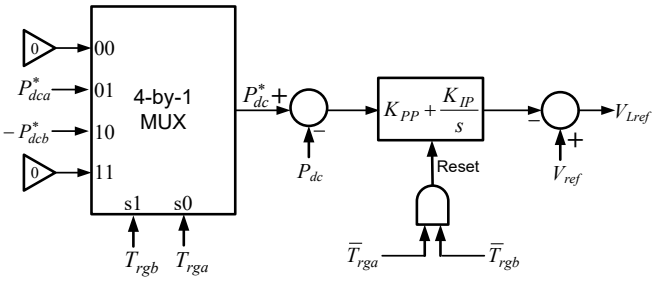

Fig. 4. DC capacitor voltage reference generation scheme.

IV. Interlinking Converter

The VSC structure of the interlinking converter used in this study is shown in Fig. 5. It is supplied from a dc storage capacitor (C_{dc}). The capacitor is connected to the DC-MG, as shown in Fig. 1. An LC filter (L_f-C_f) is connected at the output of the VSC to suppress high frequency switching harmonics. The AC side harmonics is bypassed by capacitor filter, while the dc voltages appear across capacitors, which can suppress ripples [13]. The DC voltage ripple is reduced by proper selection of L, C and switching frequency. The resistance R_f represents the converter losses. The VSC is connected to the AC-MG phases *a*, *b* and *c* through a transformer, as shown.

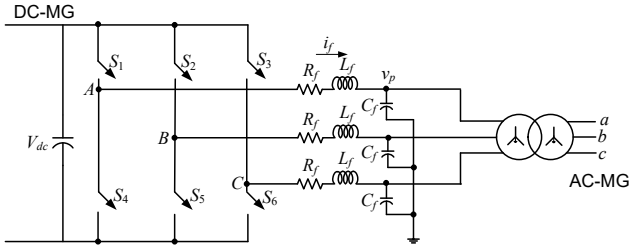

Fig. 5. Schematic diagram of the interlinking converter.

Each phase of the VSC is controlled individually through a state feedback controller that is designed taking into account the filter characteristics. Thereafter the switching signals are generated using PWM. The first step in the process is to generate instantaneous reference voltages (v_{pa}^*, v_{pb}^* and v_{pc}^*) for the three phases. The VSC switching control then has to synthesize these voltages across the filter capacitors (C_f). The reference voltage for phase-*a* is given by

$$v_{pa}^* = |V| \sin(2\pi f t + \delta) \tag{14}$$

where $|V|$ is a pre-specified voltage magnitude and δ is the desired angle. The references for the other two phases are obtained by phase shifting the above waveform by 120°.

The angle δ should be such that the required amount of power flows from the AC-MG or DC-MG. If the VSC can

regulate the voltage (V_{cdc}) across its dc capacitor (C_{dc}), the angle δ should force a power balance through feedback mechanism. Therefore, the dc capacitor control equation is given by

$$\delta_i = K_{P\delta}\left(V_{Lref} - V_{cdc}\right) + K_{I\delta}\int\left(V_{Lref} - V_{cdc}\right)dt \qquad (15)$$

V. Simulation Results

In this section, the simulation studies, performed using PSCAD, are discussed. The system parameters used in the studies are listed in Table I. The AC-MG is assumed to have a single DG with a rating of 1 MW, while there are two DGs in the DC-MG rated 500 kW and 250 kW.

Table 1: System parameters.

Quantities		Parameters
AC Side:	DG power rating	1 MW
	Frequency (f_r)	50 Hz
	Voltage L-L RMS	11 kV
	Maximum frequency Deviation (Δf)	0.5 Hz
	Droop Gain (n)	0.5 Hz/MW
DC Side:	DG-1 rating	0.5 MW
	DG-2 rating	0.25 MW
	Voltage reference (V_{ref})	2.5 kV
	Maximum frequency Deviation (ΔV)	100 V
	Droop gain for DG-1 (d_1)	0.48 Ω
	Droop gain for DG-2 (d_2)	0.96 Ω
Interlinking converter	Transformer	11/1.72 kV
	DC capacitor (C_{dc})	5000 µF
	Filter capacitor (C_f)	50 µF
	Filter inductor (L_f)	33 mH
	Switching frequency	15 kHz

A. Mode-1: Nominal Operation

In this example, it has been assumed that the AC-MG is supplying 575 kW to its local load. This is shown in Fig. 6 (a), along with the MG-AC generated power. The frequency is slightly below 50 Hz (49.92 Hz) since the DG is supplying just above its half rated power (shown in Fig. 6 b). The output of the angle controller is shown in Fig. 6 (c). Since the angle of the DG is assumed to be zero, this angle is negative to make the power flow from the DG to the load.

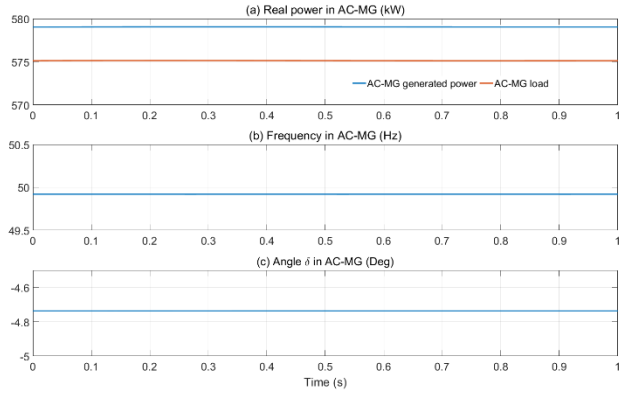

Fig. 6. System quantities in AC-MG for nominal operation.

The load in the DC side is 562 kW. This plus the losses in the DC lines are shared by the two DGs (almost) in a ratio of 2:1, as shown in Fig. 7 (a). The voltages of the DGs in the DC-MG are shown in Fig. 7 (b). It can be seen that both these voltages are above the lowest rated voltage of 2.4 kV. Also voltage V_1 is lower than V_2 since DG-1 is supplying more power than DG-2.

B. Mode-2: Power Shortfall in AC-MG

In this example, it has been assumed that the AC-MG is supplying 833 kW to the load, when at 1 s, its load demand increases to 1118 kW. Since this MG has a generation limit of 1 MW, this power has to flow from the DC-MG. Before 1 s, the local load in the DC-MG is 300 kW, which is shared by the DGs in the specified ratio of 2:1. After 1 s, the load in the DC-MG remains constant. However the generation by the two DGs increases to 288 kW and 140 kW to meet the shortfall in the AC-MG. The powers in the two sides of the hybrid MG are shown in Fig. 8.

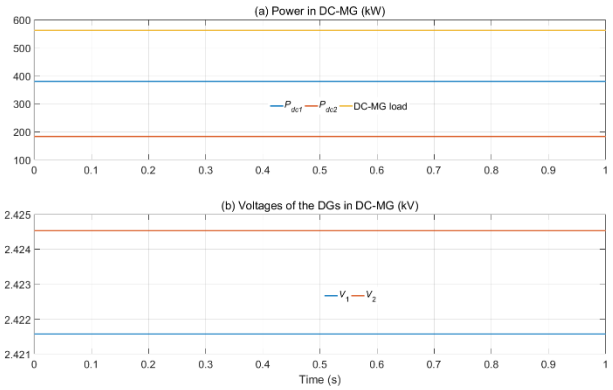

Fig. 7. System quantities in DC-MG for nominal operation.

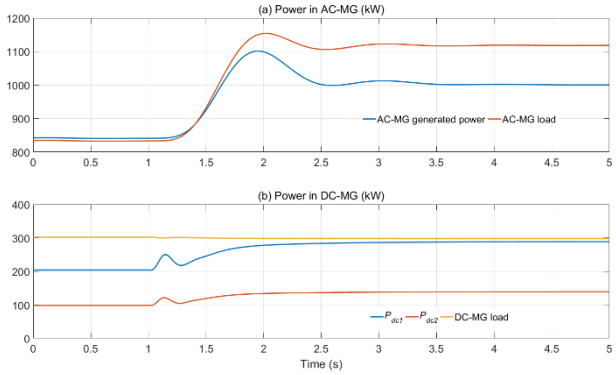

Fig. 8. Power flow through the hybrid for Mode-2.

The voltages in the DC-MG are shown in Fig. 9 (a). They remain above the lower limit of 2.4 kV. The AC-MG frequency is shown in Fig. 9 (b). It can be seen that it saturates at 49.5 Hz, as expected. The DC capacitor voltage reference is shown in Fig. 9 (c).

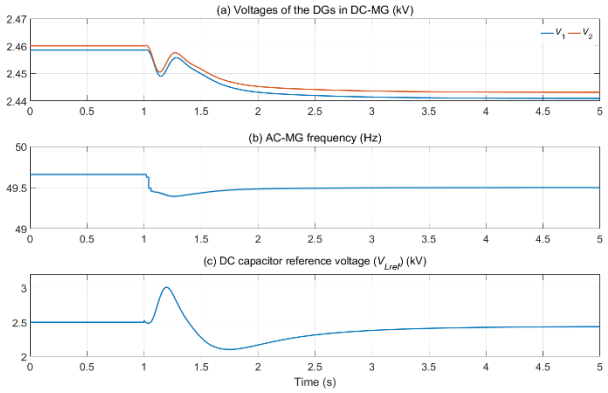

Fig. 9. DC-MG voltages, AC-MG frequency and DC capacitor voltage reference for Mode-2.

C. Mode-3: Power Shortfall in DC-MG

In this example, it has been assumed that the AC-MG is supplying 575 kW to the load such that its generation is 578.5 kW. The DC-MG is supplying 586 kW power to the load, when at 1 s, its load demand increases to 821 kW. Since the total capacity of the DGs in the DC-MG is 750 kW, the excess power has to be drawn from the AC-MG. The power flow in the AC and DC sides is shown in Fig. 10 (a) and (b) respectively. It can be seen that the AC-MG load power remains constant, while its generated power increases to 661 kW (Fig. 10 a). The DGs in the DC-MG supplies their maximum rated power, as can be seen in Fig. 10 (b).

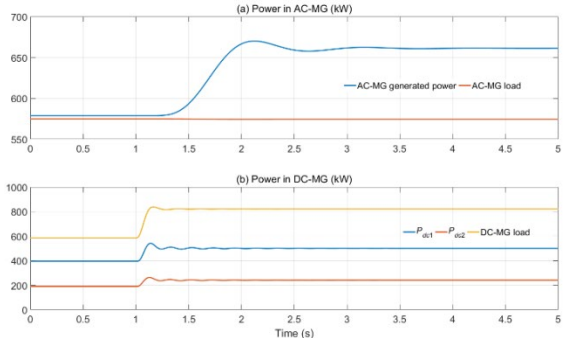

Fig. 10. Power flow through the hybrid for Mode-3.

The voltages in the DC-MG are shown in Fig. 11 (a). Since DG-1 is used for lower voltage regulation as per (12), its voltage is held constant at 2.4 kV. The DG-2 voltage is also very close to this value. The AC-MG frequency is shown in Fig. 11 (b). It can be seen that it reduces from its nominal value to accommodate for increased power generation by the AC-MG. The DC capacitor voltage reference is shown in Fig. 11 (c). The reference power that has to be drawn from the AC-MG to the DC-MG is shown in Fig. 12 (a), while the output of the angle controller is shown in Fig. 12 (b). It can be seen that the angle retards to extract more power from the AC-MG.

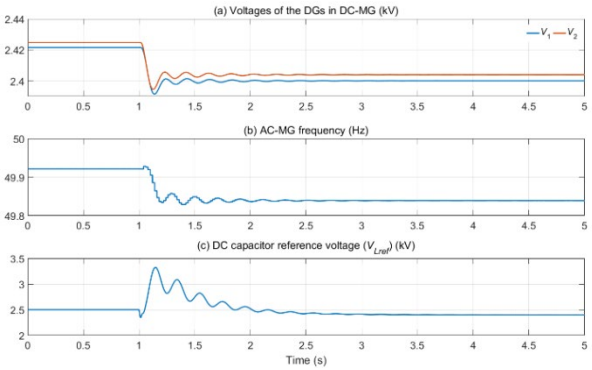

Fig. 11. DC-MG voltages, AC-MG frequency and DC capacitor voltage reference for Mode-3.

VI. Conclusions

A new method for power sharing in a hybrid microgrid without defining any droop for the interlinking converter has been proposed in this paper. Through this, the mismatch between units of the droop coefficients between the two sides of the IC has been avoided.

The proposed method introduces the use of a bidirectional power flow control switch in the DC network to control the power flow in a hybrid microgrid based only on the local measurements. The switches are controlled based on frequency in the AC side and voltage in the DC side. These signals are also utilized for the power deficiency calculations. This is advantageous since it avoids the measurements of the loads, which by nature, will be dispersed. Extensive simulation studies have been presented to verify the proposed algorithms.

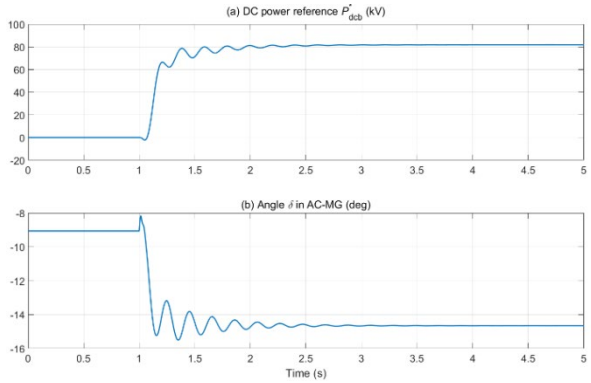

Fig. 12. DC power reference and angle controller output for Mode-3.

Acknowledgment

The authors thank the Australian Research Council (ARC) for the financial support for this project through the ARC Linkage Grant LP140100586.

References

[1] T. Ackermann, G. Andersson, and L. Söder, “Distributed generation: a definition,” *Electric power systems research,* vol. 57, no. 3, pp. 195-204, 2001.

[2] W. El-Khattam, and M. Salama, “Distributed generation technologies, definitions and benefits,” *Electric power systems research,* vol. 71, no. 2, pp. 119-128, 2004.

[3] Y. Li, D. M. Vilathgamuwa, and P. C. Loh, “Design, analysis, and real-time testing of a controller for multibus microgrid system,” *IEEE transactions on Power electronics,* vol. 19, no. 5, pp. 1195-1204, 2004.

[4] R. H. Lasseter, and P. Paigi, "Microgrid: a conceptual solution." in *PESC'04 Aachen, Germany,* 20-25 June 2004, pp. 4285-4290.

[5] N. Pogaku, M. Prodanović, and T. C. Green, “Modeling, analysis and testing of autonomous operation of an inverter-based microgrid,” *IEEE Transactions on Power Electronics,* vol. 22, no. 2, pp. 613-625, 2007.

[6] F. Katiraei, M. Iravani, and P. W. Lehn, “Micro-grid autonomous operation during and subsequent to islanding process,” *IEEE Transactions on Power Delivery,* vol. 20, no. 1, pp. 248-257, 2005.

[7] X. Liu, P. Wang, and P. C. Loh, "A hybrid AC/DC micro-grid." in *IPEC, 2010 Conference Proceedings,* pp. 746-751.

[8] P. C. Loh, D. Li, Y. K. Chai, and F. Blaabjerg, “Autonomous operation of hybrid microgrid with AC and DC subgrids,” *IEEE Transactions on Power Electronics,* vol. 28, no. 5, pp. 2214-2223, 2013.

[9] X. Liu, P. Wang, and P. C. Loh, “A hybrid AC/DC microgrid and its coordination control,” *IEEE Transactions on Smart Grid,* vol. 2, no. 2, pp. 278-286, 2011.

[10] C. Jin, P. C. Loh, P. Wang, Y. Mi, and F. Blaabjerg, "Autonomous operation of hybrid AC-DC microgrids." in *IEEE international conference on Sustainable Energy Technologies (ICSET),* 2010pp. 1-7.

[11] V. Maryama, V. Zeni, C. Q. Pica, M. S. Ortmann, and M. L. Heldwein, "Unified hybrid (Ac/Dc) active distribution networks droop-based load-sharing strategy." in *IEEE PES Innovative Smart Grid Technologies Conference Europe (ISGT-Europe)*, 2014 pp. 1-6.

[12] M. Goyal, and A. Ghosh, “Microgrids interconnection to support mutually during any contingency,” *Sustainable Energy, Grids and Networks,* vol. 6, pp. 100-108, 2016.

[13] M. Brenna, G. C. Lazaroiu, E. Tironi "High Power Quality and DG Integrated Low Voltage dc Distribution System" in *IEEE Power Engineering Society General Meeting*, 2006.pp. 6-pp